In press, Book Chapter, World Scientific

CONF-940009--1

Evolution of Rydberg States in Half-Cycle Pulses: Classical, Semiclassical, and Quantum Dynamics

Joachim Burgdörfer and Carlos Reinhold

Physics Dept., University of Tennessee. Knoxville, TN 37996-1200
and
Oak Ridge National Laboratory, Oak Ridge, TN 37831-6377

ABSTRACT

We summarize recent theoretical advances in the description of the evolution of Rydberg atoms subject to ultrashort pulses extending only a fraction of an optical cycle. We have performed classical, semiclassical and full quantum calculations in order to delineate the classical-quantum correspondence for impulsively perturbed atomic systems. We observe classical and quantum (or semiclassical) oscillations in excitation and ionization which depend on the initial state of atoms and on the strength of the perturbation. These predictions can be experimentally tested.

1. Introduction

Very recently, the generation of subpicosecond 'half-cycle' electromagnetic pulses has been achieved both in the terahertz [1] and in the gigahertz regime [2]. In contrast to short laser pulses which extend over several optical cycles, half-cycle pulses are characterized by a strong unidirectional electrical field confined to a very short time interval corresponding to only a fraction of a cycle. These characteristics make half-cycle pulses very similar to the electric field pulse generated by the passing-by projectile in an ion-atom collision. Thus, the study of the dynamics of Rydberg atoms subject to these pulses is of practical importance in problems such as transport of ions and atoms through solids (e.g. [3-4]) or plasma modelling and diagnostics of high temperature fusion plasmas ([5] and references therein). These new experimental developments have stimulated a number of theoretical studies [6-10]. From a more fundamental point of view, Rydberg atoms subject to short strong pulses provide an interesting case for the study of classical-quantum correspondence. The classical limit of quantum dynamics can formally be recovered as the limit $\hbar \to 0$. However, this limit is highly singular and non-uniform. The complexity manifests itself in the non- commutativity of the limits of long times $t \to \infty$ and $\hbar \to 0$. No matter how small $\hbar$, for times t long compared to the Heisenberg

time $t^* = \hbar/\Delta E$ where ΔE is the typical level spacing of the system, classical and quantum dynamics display discordance [11]. Since in Rydberg atoms the limit of large $n \to \infty$ is equivalent to the limit $\hbar \to 0$ and the duration of the pulse, T_p, of the order of the Heisenberg time (in a.u.) $t^* \simeq 2\pi n^3$ can be experimentally achieved, impulsively driven Rydberg atoms provide an experimental and theoretical testing ground for the classical limit of quantum dynamics. The above estimate for t^*, which agrees with the classical orbital period, T_o, is strictly valid only for a one-dimensional hydrogen atom. In the 3D case, substate splittings introduce new and longer time scales which play an important role in further delineating the classical-quantum correspondence.

We briefly review in the following results of fully classical, semiclassical, and fully quantum calculations. We illustrate the quantum-classical correspondence as a function of the pulse duration, T_p, and of the pulse amplitude and point out possible experimental tests. The dependence on the initial state is shown to be crucial in identifying the classical and semiclassical origin of oscillations in the time evolution of the Rydberg atom.

2. Theory

A hydrogen atom subject to a pulsed electric field is described by the Hamiltonian

$$H = \frac{p^2}{2} - \frac{1}{r} + F(t)z. \qquad (1)$$

where $F(t)$ denotes an external electric pulse which is directed towards the positive z-axis. z is coordinate of the electron along this axis, and $\vec{r}$ and $\vec{p}$ are the momentum and position of the electron, respectively. Atomic units are used throughout unless otherwise stated. We consider in the following a rectangular pulse $F(t) = F_p$ with $0 \leq t \leq T_p$, F_p being the peak field strength. Other pulse shapes can be treated similarly. The *classical* evolution of an electron with the Hamiltonian in Eq. 1 is calculated within the framework of a classical trajectory Monte Carlo (CTMC) approach [12]. Briefly, this approach consists of sampling a large ensemble of electronic initial conditions from a phase-space probability density which mimics the corresponding quantal position and momentum distributions of the atom and of numerically solving the cooresponding classical Hamilton equations of motion for each initial condition. The excitation and ionization probabilities can be obtained from the number of electrons which lie after the interaction with the pulse in the "target" bin of classical actions I_f around the final quantum number n_f, $n_f - 1/2 \leq I_f \leq n_f + 1/2$. Details of our initial phase-space distribution can be found elsewhere [13,14].

Our *quantum mechanical* calculations uses an expansion of the wavefunction of the electron in a basis of about 10^3 states composed of hydrogenic bound states and Sturmian pseudo states representing the continuum. Our numerical solution of the time-dependent Schrödinger equation associated with

Eq. 1 is based on the fact that the smooth field $F(t)$ can be represented by a sequence of a large number N of infinitesimal 'kicks' or instantaneous momentum transfers $\Delta p_i = T_p F(iT_p/N)/N$, i.e.

$$F(t) \simeq \sum_{i=1}^{N} \Delta p_i \delta(t - iT_p/N) \tag{2}$$

where N is increased until the ionization probability converges (typically, $10^2 < N < 10^5$) and $F(iT_p/N)$ describes the pulse shape of the field. This technique is equivalent to the split-operator algorithm for the calculation of the evolution operator [15]. If $U(t_{k+1},t_k)$ denotes the evolution operator that evolves the state of the electron $|\Psi(t)\rangle$ from an instant of time $t_k = kT_p/N$ just before the k^{th} kick to an instant of time t_{k+1} just before the $k+1^{th}$ kick, then

$$U(T_p,0) = \prod_{k=0}^{N-1} U(t_{k+1},t_k) \tag{3}$$

with

$$U(t_{k+1},t_k) = e^{-iH_0 T_p/N} e^{iz\Delta p_k} \tag{4}$$

where H_0 is the unperturbed Hamiltonian of the atom. A more detailed description of the method can be found elsewhere [16].

Unlike our classical and quantal calculations, the semiclassical analysis is performed for an effectively one-degree of freedom problem. We use the semiclassical S matrix formulation of Miller [17]. The transition amplitude from an initial state n_i to a final state n_f is given by

$$t^{sc}_{n_i,n_f} = \sum_i \left(\frac{1}{2\pi i} \frac{\partial I(t_f)}{\partial \theta_i} \right)^{1/2} \exp\left[-i \int_0^{t_f} dt [E(t) + \theta(t) \frac{dI(t)}{dt}] \right] \tag{5}$$

where $I(t)$ is the action of the classical orbit starting at t=0 with a value $I(0)=n_i$ and ending at the conclusion of the pulse with $I(t_f=T_p)=n_f$. The conjugate angle is denoted by θ and the sum extends over all initial angles ϑ_i which serve as starting points of trajectories connecting the integer values n_i and n_f. If more than the one path connects n_i and n_f, semiclassical path interferences occur. The action-angle variable representation is valid only for bound-bound transitions. However, ionization probabilities can be estimated from the probability flux to very high $n_f >> n_i$ for times $t \leq T_p$. Eq.(5) represents the primitive, i.e. non-uniform semiclassical approximation. It does not contain contributions from dynamical tunneling and possesses unphysical singularities at caustics.

The semiclassical approximation (Eq.(5)) is only valid in those cases for which the $3D$ classical mechanics is effectively dynamically confined to one "reaction coordinate" which turns out to be the parabolic coodinate $\eta = r - z$ and which describes the motion across the potential barrier of the time-dependent Stark effect. We employ 3D classical trajectories but include only those for which the other parabolic coordinate, $\zeta = r + z$, remains small compared to the

size of the orbit during the evolution. In terms of parabolic actions (or quantum numbers) we choose the maximum value $n_2(t=0)=n-1$ and the minimal value $n_1(t=0)=0$. We include all conjugate initial angles θ_1 and θ_2 which lead to the desired outcome of an effective quasi- one dimensional transition to $I_2(t=T_p)=n_f-1$ and $I_1(t=T_p)=0$. In our $3D$ calculation the final action $I_1(T_p)$ is not exactly zero, and we accept the trajectories as a desired outcome provided $I_1(T_p)$ lies in a bin near zero, $I_1(T_p)\leq 0.5$. The action-angle variables entering explicitly the one-degree of freedom formula (Eq.(5)) are therefore I_2 and θ_2.

The approach to the *classical limit* starting from Eq.(5) involves two steps. One first disregards all cross terms in the double sum over classical paths in the probability $P_{n_i,n_f}=|t_{n_i,n_f}|^2$ based on the argument that is the limit $\hbar\rightarrow 0$ they oscillate infinitely rapidly. This amounts to an averaging over a small interval of the final action I_f whose size tends to zero as $\hbar\rightarrow 0$. The classical limit is given by an incoherent sum over contributions from all pathes

$$P_{n_i,n_f}=\frac{1}{2\pi}\sum_i\left|\frac{\partial I(T_p)}{\partial\theta_i}\right|. \qquad (6)$$

The classical Monte Carlo method is recovered from Eq.(6) by summing over all events for which the final action is not a well-defined integer but lies in the interval $n_f-1/2\leq I(T_p)\leq n_f+1/2$. This "binning" can be made to preserve microreversibility if both initial and final actions are binned in a symmetrical form. It should be noted that only in the limit $\Delta I_{f,i}/n_{f,i}\rightarrow 0$ the CTMC method is asymptotically equivalent to the classical limit of vanishing bin size (Eq.(6)). For large but finite n the equivalence is only approximate. "Binning" corresponds to an averaging over $I_{i,f}$ of probabilities (as opposed to amplitudes).

3. Stark beats

The excitation dynamics of the Hamiltonian (Eq.1) depends strongly on the initial state. We stress the fact that the origin of semiclassical (or classical) oscillations in the excitation function are different for initial states which are spherical eigenstates $w_{n\ell m}$ of the zero-field Hamiltonian and those which are eigenstates of the Stark Hamiltonian in presence of a static electric field. i.e. parabolic states $\psi_{n_1n_2m}$. The reasons for the difference are twofold: spherical states are. unlike parabolic states. intrinsically three-dimensional and the reduction in terms of one "reaction coordinate" is not valid. In fact. only one extreme parabolic state which resides near the saddle (see Fig. 4 below) can be approximated in terms of an effective 1D system. The second reason is the presence of additional Stark "beat" frequencies due to the lifting of the n shell degeneracy which introduced new time scales larger than the 1D Heisenberg time $t^*=2\pi n^3$. These Stark oscillations tend to overshadow oscillations due to

the coupling of different n levels, or equivalently, of path interferences between n changing trajectories.

Excited states of hydrogen with energy levels $E_n=-1/(2n^2)$, are energetically split due to the linear Stark effect

$$E_{n_1,n_2} = E_n+\tfrac{3}{2}n(n_1-n_2)F, \tag{7}$$

where n_2,n_2 denote parabolic quantum numbers ($n=n_1+n_2+|m|+1$,m being the magnetic quantum number). Accordingly, the wavefunction of hydrogen prepared in an initial state $|n_i,\ell_i,m\rangle$ and exposed to a half cycle pulse, $F(t)$, during a time interval $0<t<T_p$ is given in the limit of weak fields by

$$|\Psi(T_p)\rangle\simeq\exp(-iE_n\tau)\sum_{n_1,n_2}\langle n_1,n_2,m|n_i,\ell_i,m\rangle|n_1,n_2,m\rangle \exp[-i\tfrac{3}{2}n(n_1-n_2)\Delta p] \tag{8}$$

where the sum extends over all parabolic states within the shell n_i. In the following we focus on $m=0$ for the polarization of the fields (laser and half-cycle pulse) parallel to the z axis. The evolution phase accumulated between $t=0$ and $t=T_p$ depends on the time integral over the field strength

$$\Delta p = \int_0^{T_p} dtF(t) \tag{9}$$

(the product F_pT_p for a rectangular pulse if $F(t)=F_p$ for $0\leq t\leq T_p$) rather than the field strength and the time separately. In the limit of ultrashort pulses, the variable Δp represents the momentum transferred to the electron by the pulse.

The expectation values of dynamical variables $\langle\Psi(t)|A|\Psi(t)\rangle$ display oscillations as a function of time ('Stark beats') due to the time evolution factors $\exp(\pm i\Phi_{n,k})$ ([18] and references therein)

$$\Phi_{n,k}(\Delta p) = 3nk\Delta p = 3nkF_pT_p \qquad k=1.2....(n-|m|-1). \tag{10}$$

The precondition for the appearance of Stark oscillations is that the initial state is a *coherent superposition* of different eigenstates of the Stark Hamiltonian, i.e. of different parabolic states (see Eq. (8)). A spherical state $w_{n\ell m}$ is a realization of such a coherent superposition.

The appearance of Stark beats as a consequence of coherent superposition of quantum states should not obscure the fact that Stark beats are of semiclassical, those with the fundamental period even of classical origin [18]. Beats with the fundamental period are described by secular perturbation theory for adiabatic invariants [19]. We use the two classical pseudospin vectors

$$\vec{j}_{1,2} = \tfrac{1}{2}\left(\vec{L}\pm\vec{a}\right) \tag{11}$$

which are linear combinations of the angular momentum $\vec{L}$ and the normalized Runge-Lenz vector $\vec{a}=\frac{n}{Z}\vec{A}$ where

$$\vec{A}=\vec{p}\times\vec{L}-Z\frac{\vec{r}}{r}. \tag{12}$$

In the presence of a weak electric field, $\vec{F}$, the two pseudospin vectors precess about the electric field vector according to the Bloch equations (Fig. 1),

$$\begin{aligned}\frac{d}{dt}\vec{j}_1 &= \vec{\omega}\times\vec{j}_1 \\ \frac{d}{dt}\vec{j}_2 &= -\vec{\omega}\times\vec{j}_2\end{aligned} \tag{13}$$

with

$$\vec{\omega}=\tfrac{3}{2}n\vec{F}. \tag{14}$$

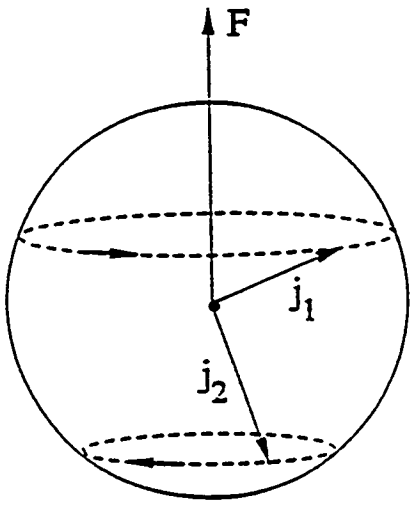

Fig. 1: Precession of the classical pseudospins $\vec{j}_{1,2}=\frac{1}{2}(\vec{L}\pm\vec{a})$ about the electric field $\vec{F}$ vector.

In view of Eq.(11), the pseudospin precession results in a periodic fluctuation in $\vec{L}$ and $\vec{A}$. If at t=0 the two pseudospins lie in the $x-z$ plane and with $j_{1,x}>0$ and $j_{2,x}>0$ the vector $\vec{L}$ has its maximum length $|\vec{L}|$. At $t=\frac{\tau}{3nF}$ the two vectors $\vec{j}_1$ and $\vec{j}_2$ have precessed into the $y-z$ plane pointing in opposite directions ($j_{1,y}<0$, $j_{2,y}>0$ or vice versa). In this configuration the length of $\vec{a}$ has reached its maximum value while $|\vec{L}|$ is at its minimum. After a period of $t_s=2\pi/\omega_s=\frac{2\pi}{3nF}$,$|\vec{L}|$ has reached its second maximum, with the two pseudospin lying in the $x-z$ plane and both x components $j_{1,x}, j_{2,x}$ negative.

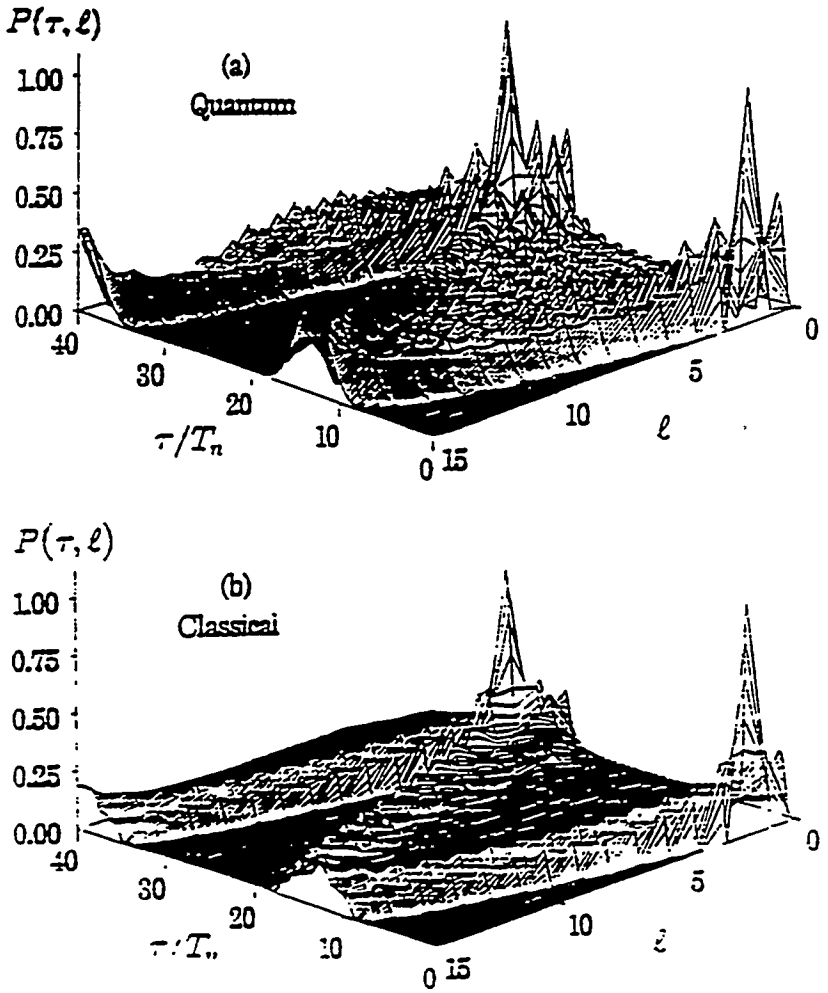

Fig. 2: Time evolution of the population of all ℓ states in the n=16 manifold after $H(16d_0)$ is exposed to a rectangular pulse with F_p=1kV cm^{-1}: quantum (a) and classical (b).

This recurrence time corresponds to the fundamental Stark period (or beat frequecy ω_s=3nF (see Eq. (10)). Fig. 2 displays both the quantum and classical evolution of a initial 16d m=0 state in hydrogen in angular momentum space under an influence of a half cycle pulse with a strength F_p=1 kV/ cm in the perturbative regime. While the fundamental beat periods for Stark beats with frequency ω_s of the wavepackets agree very well, the quantal evolution shows oscillations with all 15 harmonics (k=1,... $n-|m|-1$). This frequency spectrum can be recovered by semiclassical quantization of the pseudospins $\vec{j}_{1,2}$.

It can be shown that the Stark-like beat pattern persists for much higher field strength well into the regime of overlapping n manifold ($F \gtrsim F_c = \frac{1}{3}n^{-5}$ or equivalently, and for a scaled field $F_0 = \frac{1}{3n}$, where $F_0 = Fn^4$). For short pulses. it also applies to non-hydrogenic systems, as long as the avoided crossings are still predominately traversed diabatically [18]. The experimentally observed oscillations in the survival probability of Na(16d) for pulses with $F_p \leq 10$kV/cm [20] can therefore be identified as Stark beats.

4. Oscillations in the Excitation Probability of Parabolic States

When adjacent n manifolds strongly overlap, oscillations with frequencies associated with the energy spacing $\Delta E_n = n^{-3}$ and the 1D Heisenberg time begin to show up. However, they are overshadowed by the large number of Stark frequencies. A different situation occurs for parabolic initial states and strong fields. Parabolic states diagonalize the evolution operator for a static field. Therefore, the coherent superposition (Eq.(8)) and the Stark beats are absent and only couplings between different n manifolds govern the spectrum of oscillation frequencies in the excitation function. Because of the dynamical symmetry of hydrogen in a presence of an electric field, the number of couplings is. however, limited. Most of the crossings between states of different n manifolds are strictly diabatic. The most "redshifted" Stark state ($n_2 = n-1$, $n_1 = 0$) with the lowest energy and which lies closest to the potential saddle plays an exceptional role. After traversing all other states of the adjacent lower manifold $n' = n-1$ diabatically, this state undergoes a broad avoided crossing with the lowest member of the n' manifold with quantum number $n_2' = n'-1$ and $n_1' = 0$. The avoided crossing occurs at a field strength close to static field ionization threshold $F_c \simeq 1/9n^4$ (or $F_0 = 1/9$). Near this broad avoided crossing strong couplings to many other n levels and to the continuum occur. At this field strength which is large compared to the Stark beat regime ($F \lesssim \frac{1}{3n^5}$) the excitation function of the extremal ("downhill") state possesses oscillations which are associated with path interferences [8] between different n changing pathes. It is the proximity in both energy and coordinate space to the saddle that renders the dynamics quasi-one dimensional with the parabolic coordinate $\eta = r - z$ as reaction coordinate. Path interferences can therefore be described in terms of the one-dimensional semiclassical transition matrix (Eq.(5)).

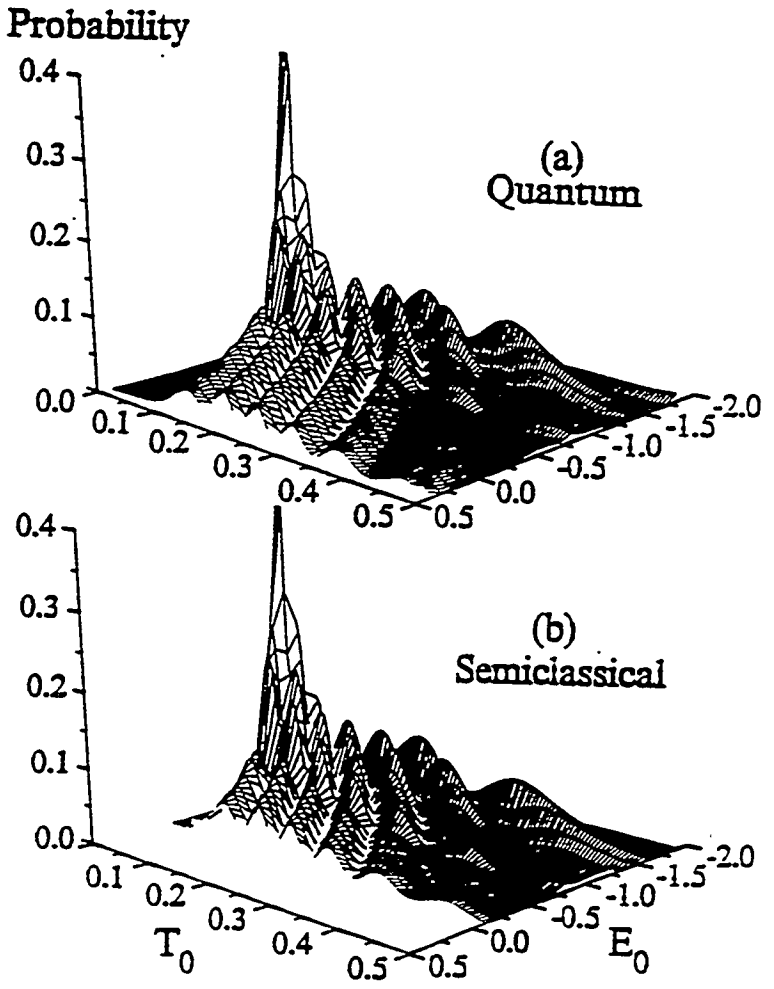

Fig. 3: Quantum (reduced basis set) and semiclassical population dynamics of excited states of a hydrogen atom initially in a "downhill" n=20.n_2=19.m=0 state as a function of time. Binding energy and time are expressed in units of the initial ionization potential and orbital period, respectively (E_0=$E/|E_{ni}|$,T_0=T_p/T_{ni}).

Fig. 3 presents the comparison for the time evolution in energy space of an initial n=20.n_2=19 state in the presence of a electric field of F=5×10^{-6} a.u. (scaled field F_0 = 0.8) using both the semiclassical transition matrix (Eq.(5)) and the solution of the Schrödinger equation. Since the dynamics is quasi- one-dimensional we have included only the n_1=0 states in a reduced basis which allows to subtend both the near threshold regime and the continuum with a finer energy grid as compared to the full 3D calculation. In the

semiclassical calculation we have removed the singularities which are caused by the primitive (i.e. non-uniform) treatment of the caustics. The agreement between the semiclassical and quantal calculation is very good. While in its current form (Eq.(5)) not directly applicable to ionization, the semiclassical analysis has the advantage that the origin of the oscillations can be understood as an interference between one path approaching the nucleus with high speed and being strongly perturbed by the field and another path starting close to the saddle and being driven to other n or even to the continuum by the time-dependence of the saddle potential (Fig. 4). The oscillations observed in Fig. 3 extend to positive energies $E>0$ indicating that not only bound state excitation but also the ionization probability displays oscillations as a function of time or field strength. On the other hand. ionization of the other extreme parabolic state ($n_2=0, n_1=n-1$), the most blue shifted or "uphill" state, does not display oscillations in the ionization probability as a function of F. This state resides near the repulsive wall (Fig. 4). The classical orbits in the region of phase space are not confined to one reaction coordinate but explore the plane perpendicular to the field direction. The simplified 1D semiclassical analysis (Eq.(5)) is therefore not applicable. The 3D classical dynamics features, however, classical beats as a function of the time with the period of the Heisenberg time t^*.

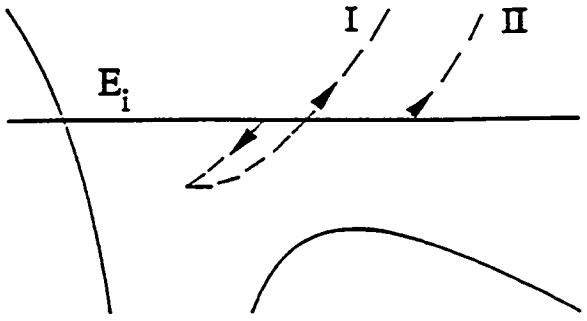

Fig. 4: Typical interfering trajectories leading to ionization of the quasi-one-dimensional "downhill" state of hydrogen in a strong electric field. E_i: initial orbital energy, solid line: instantaneous potential in the field $F(t)$ along the z coordinate. schematically.

It is important to realize that the semiclassical path interference can be observed only for pulse durations comparable to the classical orbital period. In the ultrashort pulse limit ($T_p \to 0$) the energy and momentum transfer is purely impulsive,

$$\Delta E = \Delta p^2/2 + \vec{p}(r)\vec{\Delta}p \tag{15}$$

and the solution of Eq. (15) is unique, i.e. only one initial condition $\vec{r}$ for the trajectory features the correct orbital momentum $\vec{p}$ to transfer the required energy ΔE. In this impulsive limit ionization becomes completely classical provided that the momentum transfer Δp is sufficiently large [6,21].

5. Discussion

We have delineated two distinct regimes in which excitation and ionization of Rydberg atoms by short electric half-cycle pulses displays oscillations. One regime refers to spherical initial states and field strength comparable to fields sufficient for n manifold overlap ($F \approx \frac{1}{3n^5}, F_0 = \frac{1}{3n}$), the other to one extreme parabolic initial state and field strengths near the static ionization threshold ($F \approx F_0/9$). In each case some (but not all) oscillatory structures indicate that quantum mechanics or semiclassical mechanics diverges from classical mechanics since the time scales involved are of the order of the Heisenberg times t^* where the existence of discrete energy levels leaves its mark on the dynamical evolution. On the other hand, in the impulsive limit, $T << t^*$, classical mechanics can mimic quantum dynamics quite well. Short times are, however, only a necessary but not a sufficient condition. A second condition to be fulfilled is that the transfer of momentum Δp must be sufficiently large [21].

$$\Delta p n^2 \gg 1 \tag{16}$$

This relation can be simply understood in terms of the uncertainty principle. The De Broglie wavelength $\lambda = 1/\Delta p$ associated with the momentum transfer should be small compared to the size of the orbit ($\propto n^2$). In this limit the internal structure of the atom is resolved and the energy transfer proceeds via localized interactions between the electron and the field conserving energy and momentum, rather than by classically forbidden dipole transitions by virtual photon absorption. The predictions of the present theory can be tested by current experiments [1,2] and should provide detailed insight into classical-quantum correspondence and the approach to the classical limit.

The authors acknowledge illuminating discussions with J. Delos, R. Jones, and C. Schwieters. Work supported in part by the National Science Foundation and by the U.S. Department of Energy, Office of Basic Energy Sciences, Division of Chemical Sciences, under Contract No. DE-AC05-840R21400 with Martin Marietta Energy Systems, Inc.